

pubs.acs.org/NanoLett Letter

Optical Trapping and Positioning of Silicon Nanowires via Photonic Nozzling

Matthew Eliceiri and Costas P. Grigoropoulos*



Cite This: Nano Lett. 2022, 22, 3777-3783



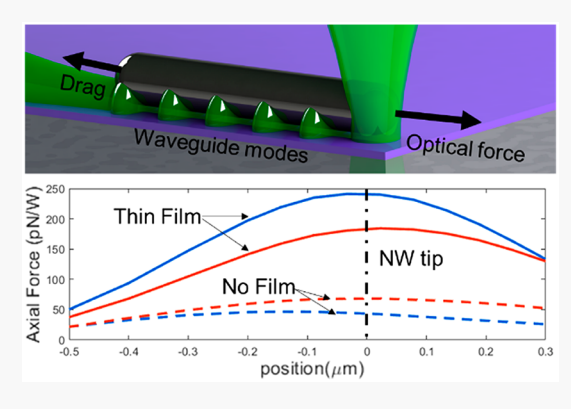
ACCESS I

Metrics & More



SI Supporting Information

ABSTRACT: We have improved the maximum two-dimensional translation rate of optically tweezed silicon nanowires to 30 μ m/s while lowering the power usage by an order of magnitude from the ~100 mW range to 6 mW using a silicon film substrate at 532 nm laser wavelength. We then explain the mechanism for the enhanced tweezing using finite difference time domain simulation as "waveguide nozzling" of the incident radiation, directing the light underneath the nanowire where it is confined and forced to propagate opposite to the direction of nanowire motion. We then demonstrate the robust and deterministic placement of the nanowires on the Si film surface using a nanosecond laser at the same wavelength.



KEYWORDS: silicon nanowire (SiNW), optical tweezers, photonics

1. INTRODUCTION

The most critical issue inhibiting the integration of bottom-up nanostructures into scalable applications is the inability to reliably organize and position them on demand. Currently deployed nanoscale consumer devices are almost exclusively produced lithographically. Certainly, this may be an optimal strategy for many devices, but to explore and expand possible applications of bottom-up technologies, physical positioning of structures must be mastered beyond the current state of the art. One method of positioning that has attracted certain attention is optical tweezing. $^{1-3}$ Optical tweezing has two steps. First, a stable optical trap wherein the radiation pressure force exhibits negative feedback with respect to position on a particle must be created. Second, the trapping focal point must maintain a sufficient pressure force to resist both the Brownian motion and drag force as the particle is translated through the trapping fluid medium. While these criteria are easily met for transparent particles larger than several microns, nanostructures are significantly more difficult to tweeze. The principal cause for this is that optical trapping forces scale with particle volume on the nanoscale, making it very difficult to generate large optical forces with small objects. 1D nanostructures may provide a significant advantage in this respect, as will be demonstrated in this work.

Previous work in the optical trapping of nanowires (NWs) has relied principally on complex beam shaping methods, including computer generated holograms and Bessel beams. Scanning speeds of at most $10-20~\mu\text{m/s}$ for semiconductor NWs have been reported using laser powers on the order of 100~mW. Additionally, previous work has employed oil

immersion with high numerical aperture lenses.^{5–7} The use of beam shaping and high aperture optics, however, comes with a significant increase in experimental complexity. Additionally, the use of higher power lasers presents other issues, including unwanted heating, liquid boiling, and target damage as well as power consumption, laser cost, and safety concerns. Eliminating these challenges will allow for easier integration of NW optical tweezing where it was not previously feasible, such as in temperature sensitive biological applications, applications with restrictions on aperture, or significant cost restrictions.

Previous investigators examined the optical effects of bringing silicon nanowires (SiNWs) near a reflecting surface for tuning the spectral scattering of SiNWs. With the SiNW near the surface of an aluminum mirror, light was irradiated onto the reflector surface causing standing waves between the SiNW and the surface. The interaction between these standing waves and the SiNW resulted in strongly enhanced Mie resonances in the nanowire and allows for spectrally selective scattering. The observed resonance effects by the SiNW-reflecting surface tandem were quantitatively linked to the quantum Purcell effect. In our study, we will show that this enhancement of optical fields surrounding a SiNW using a

Received: March 1, 2022 Revised: April 14, 2022 Published: April 19, 2022





Nano Letters pubs.acs.org/NanoLett Letter

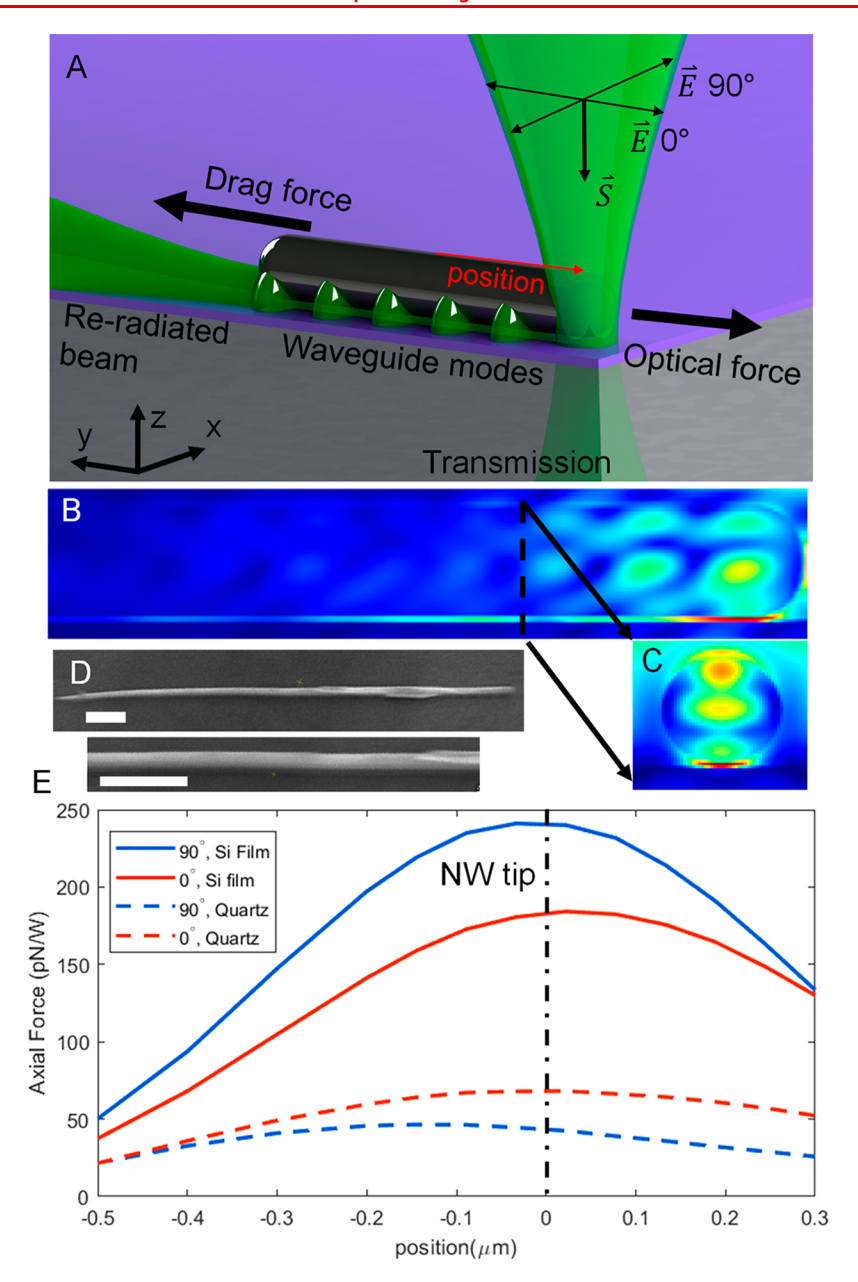


Figure 1. Optical trapping setup and simulation for 200 nm diameter SiNW. (A) Diagram of optical force and drag force directions relative to the nanowire. Light comes from above, then redirects underneath and through the nanowire in the +y direction, inducing a force in the -y direction. Nanowire motion is in the direction of optical force. Angular indication above the green laser indicates convention for polarization. (B) E-field intensity plot cut lengthwise through SiNW with a broken line to indicate the cross section shown in C. (C) E-field intensity cross section 470 nm from a trapped SiNW tip showing field enhancement beneath the SiNW. (D) Example image of single SiNW of 180 nm in diameter; scale bars are 1 μ m. (E) Optical forces simulated along the axial direction for four different substrates and polarization conditions.

reflecting surface can significantly increase the efficiency of the optical tweezing of 1D nanostructures.

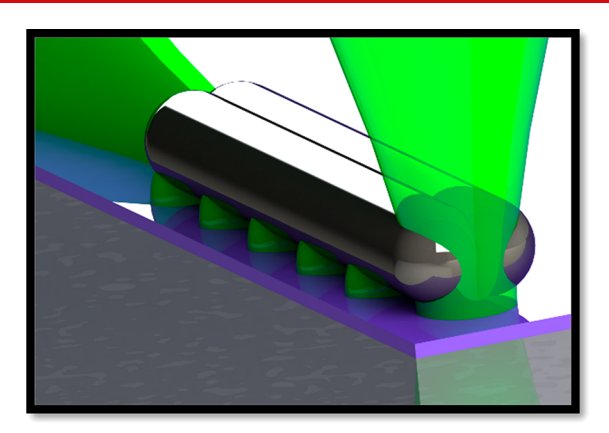
In this work, we present a significant improvement at the expense of sacrificing translation in the direction of the optical axis. For many applications, this will be a minor concession, as most nanoscale devices and structures are assembled on a two-dimensional platform, i.e., a chip, wafer, or slide, and our method can therefore be easily implemented in most configurations. We optically tweeze SiNWs with a low aperture lens at powers an order of magnitude lower than previously demonstrated, maintaining or improving scanning speed with a simple Gaussian beam by confining the trap to the vicinity of the surface of an amorphous silicon (a-Si) thin film. We show that this tweezing method achieves strongly improved optical

force due to what we refer to as the nozzling effect, where the NW serves as an efficient waveguide, directing radiation away from the trapping site, inducing a force in the direction of translation. We further show that we can easily place suspended nanowires in a specific location and orientation, and that the resulting pattern withstands drying.

2. RESULTS

Optical Tweezing. We performed optical tweezing of SiNWs using a continuous wave (CW) 532 nm wavelength laser focused via a Mitutoyo 20X long working distance objective with a numerical aperture of NA = 0.42. The SiNW synthesis has been described in depth previously. SiNWs were dispersed in deionized water on a covered quartz slide

Nano Letters pubs.acs.org/NanoLett Letter



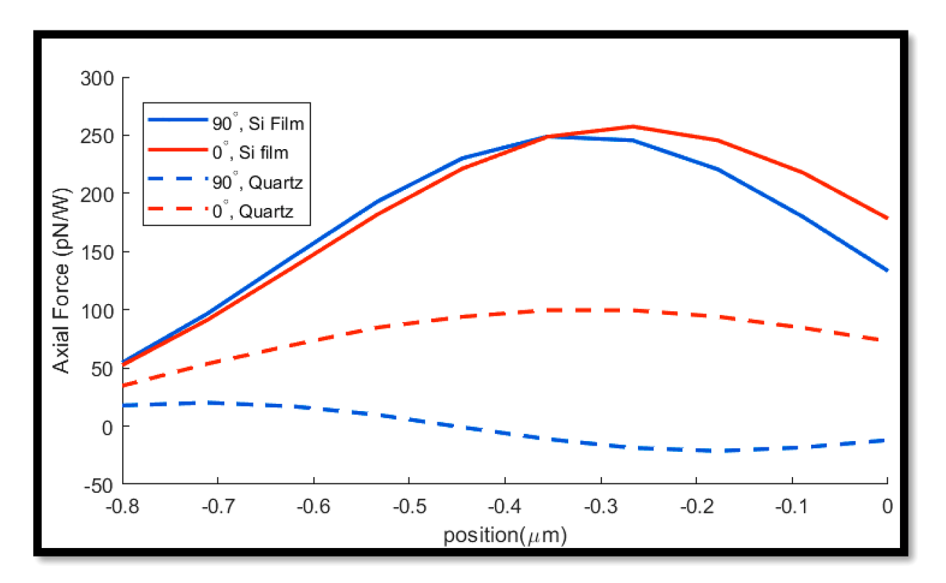


Figure 2. SiNW bundle trapping optical force parameter sweep displaying axial optical forces as a function of distance from the focus to the SiNW tip for the modified SiNW geometry. Top: geometric layout of the two-nanowire bundle modeled, with the wire centers overlapping with the opposing wire's edge.

with a 30-nm-thick a-Si film deposited on the quartz. The deposition and etching have also been described previously. The water level was approximately 100-µm-thick. The measured power of the CW beam was varied between 2 and 11 mW. The maximum scanning speed we achieved was 30 μ m/s and is documented in video format in Supporting Information video S1 at 5 mW CW laser power. Additionally, we tested the effect of scanning the tweezed SiNW off the edge of the silicon film, shown in Supporting Information videos S2 and S3. In these videos, the wire was scanned at 15 μ m/s in one direction until the wire reached the end of the film. Evidently, the wire is easily trapped and translated when over the a-Si film. Once the edge of the film is reached, the trap is immediately broken. The behavior observed in these videos was highly repeatable, and there were no cases of stable trapping away from the a-Si film. In Supporting Information video S4, we show the smallest single SiNW we were able to stably trap and scan. While the larger nanowires scanned may be composed of nanowire bundles, the single nanowires are in the range of 150-300 nm in diameter with a circular cross section and slight variation in cross sectional size over the length. Example SEM images of single SiNWs are shown in Figure 1D. This scanning speed is 15 μ m/s with 6 mW of power, still 1 order of magnitude lower power than previous optical tweezing setups.⁵⁻⁷ The wires can also be easily

oriented since they align along the motion direction. Therefore, by navigating the SiNW such that it arrives at a specified location with a desired velocity orientation, we can position the wire at any arbitrary 2D position and orientation.

Additionally, we tested experimentally whether other nanowires could be tweezed and whether other films could be used. Supporting Information video S5 shows the tweezing of a 150 nm diameter silver nanowire with 6 mW of power on the a-Si film, achieving the highest speed observed at 60 μ m/s, and Supporting Information video S6 shows the tweezing of SiNWs on 100-nm-thick Al film, achieving a 10 μ m/s translational speed at 6 mW of power. We therefore demonstrate that we can tweeze nanowires and substrates of different materials; however we reserve deeper analysis of these alternate material scenarios for future work to fully describe the process for SiNWs.

To understand why we observe strong trapping enhancement, we performed finite difference time domain simulation (FDTD) using Lumerical software with a layout diagrammed in Figure 1a. We assumed a small separation distance of 5 nm between the wire and the substrate. We anticipate that the downward radiation pressure on the wire will press it close to the substrate, and at a distance in the proximity of 5 nm the van der Waals forces will dominate, bringing the wire into contact with the substrate. ^{12,13} A previous study on the

Nano Letters pubs.acs.org/NanoLett Lette

stability of silica and silicon nanoparticles, however, has shown that hydroxyl groups on the surface of the particles will create an electrostatic repulsion force and prevent the particles from sticking to the substrate or to each other. 14-16 Knowing the vertical force on the wire from preliminary simulation, we balance the thermal equipartition energy against the vertical radiation pressure force to obtain a measure of the offset distance. This calculation yields a gap distance between 3 and 5 nm, and for all simulations this gap was set to 5 nm. We modeled the NW as a 200-nm-diameter, 5-µm-long cylinder with hemispherical end-caps. Further simulation parameters are given as Supporting Information. We include outputs of the E-field down the length of the NW and a cross-sectional view in Figure 1b,c. It is clear from these plots that there is strong enhancement of the electric field underneath the wire. By redirecting the radiant energy from the incident beam with no momentum into the direction of the SiNW axis to underneath and through the wire, maximizing the axial momentum, an efficient optical force is generated by conservation of momentum as diagrammed in Figure 1a. Because the drag force will immediately align the nanowire in the direction of SiNW motion, we will observe a very strong trapping force in the direction of tweezer scanning. This redirection of radiation therefore functions as a photonic nozzle for the nanostructure in motion, directing the radiative impulse only in the desired direction to counteract the drag force and maximize translational velocity.

Selectively scattering the radiation incident from above the nanowire to directly opposite the direction of drag force gives the most efficient optical tweezing. It is therefore beneficial to increase the coupling of the incident light to these axially propagating modes. In our case, the incident radiation will couple into the resonant gap between the reflective a-Si film surface and the nanowire surface. A previous study has shown that the presence of a reflective surface near the SiNW strongly enhances the local density of optical states beneath the nanowire,8 which therefore increases the chance for incoming radiation to couple into these confined modes. To verify the optical forces via simulation, we modeled the trapping force for four different cases: with and without a silicon film underneath the nanowire, each modeled with the electric field polarization either parallel or perpendicular to the nanowire. We repeated the simulation for 10 offset distances, measured from the central focus of the incident beam along the nanowire axis to the tip of the nanowire as indicated by the red arrow in Figure 1A. The results of this parametric sweep are shown in Figure 1E. Both polarizations induce a strong axial force with the film present, and an order of magnitude lower force without the film. This closely matches experimental observations as the nanowire trap very clearly stops functioning as it is scanned off the Si film patch and onto the bare quartz substrate. To better visualize the redirection of the radiation, we have included a video of the electric fields over time for the simulation performed in Figure 1 at position = 0 μ m, and a polarization of 90°, with the silicon film. In video S7, we displayed the electric field magnitude from a cross-section parallel to the silicon substrate and halfway between the SiNW and the substrate. Video S8 shows the same electric fields from a section cut along the SiNW axis. From video S7, the propagation of the wave along the NW gap is evident from the oscillations caught in a single line down the center of the screen where the SiNW lies, and in video S8 the additional modes through the body of the SiNW are also apparent along with the enhancement underneath the wire.

Some of the nanowires shown in the figures and videoed in the Supporting Information appear to be composed of nanowire bundles. For this reason, we briefly examine the effects of nanowire bundles in the simulation. We performed a simulation identical to that performed for optical forces in single nanowires but added a second overlapping nanowire. The result is shown in Figure 2. Very similar to Figure 1E, the optical forces on the two-nanowire bundle are very strong for both polarization cases with the silicon film and low or even negative with a bare quartz substrate. Due to the robustness of the trapping force enhancement under changes to the nanowire geometry as well as the strong experimental evidence of efficient trapping, the photonic nozzling is effective for both single silicon nanowires as well as silicon nanowire bundles.

Additionally, we must explain why the nanowire exhibits stable trapping at zero velocity. For a perfectly symmetric SiNW, it is only possible to stably trap at a center of symmetry. Experimentally, however, it is clear there is stable trapping at the tip even with no motion. This is caused by the inherent asymmetry induced during the nanowire synthesis. The bottom right inset SEM image in Figure 3 shows a pronounced

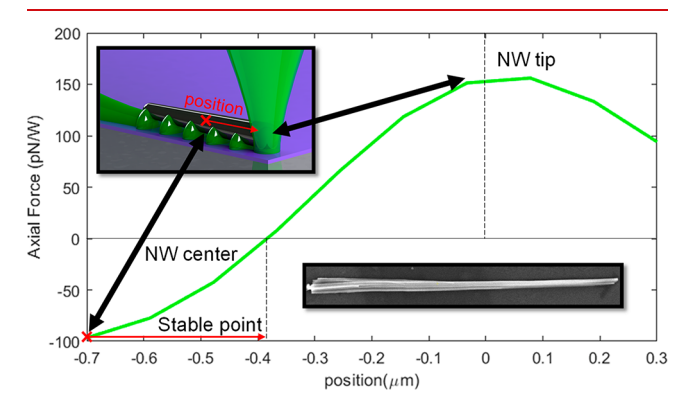


Figure 3. Optical force simulation result showing stability of the optical trap for slightly conical nanowires 200 nm in diameter with a 1° conical angle, position again measured from the SiNW center. The stable point where nozzling force balances asymmetry induced force is indicated by red arrows. Bottom right inset shows an image of an example SiNW with a large asymmetry in thickness, with a length of 16.8 μ m.

case of this asymmetry, with one end clearly thicker than the other and a conical angle of approximately 2° measured from the image. We modeled SiNW asymmetry via FDTD using a truncated cone with a 1° conical angle and found that there is a stable point as indicated 0.38 $\mu \rm m$ from the wire's thicker end. The optical force will be reduced upon irradiating the thicker end; however this force is balanced at some point by the waveguide nozzling effect discussed above, resulting in a nanowire stably trapped near the tip, matching experimental observations. The stability is indicated via the sign change in optical force in Figure 3.

Positioning and Stiction. The final objective of our study was to investigate whether the SiNWs could be deterministically placed, oriented, and then fixed in position rigidly enough to withstand drying. To do this, we irradiated the SiNW with a 3 ns, 532 nm pulsed laser, inducing rapid water vapor expansion and collapse. After this, the wire was no longer suspended in the liquid but stuck to the surface. The entire

Nano Letters pubs.acs.org/NanoLett Letter

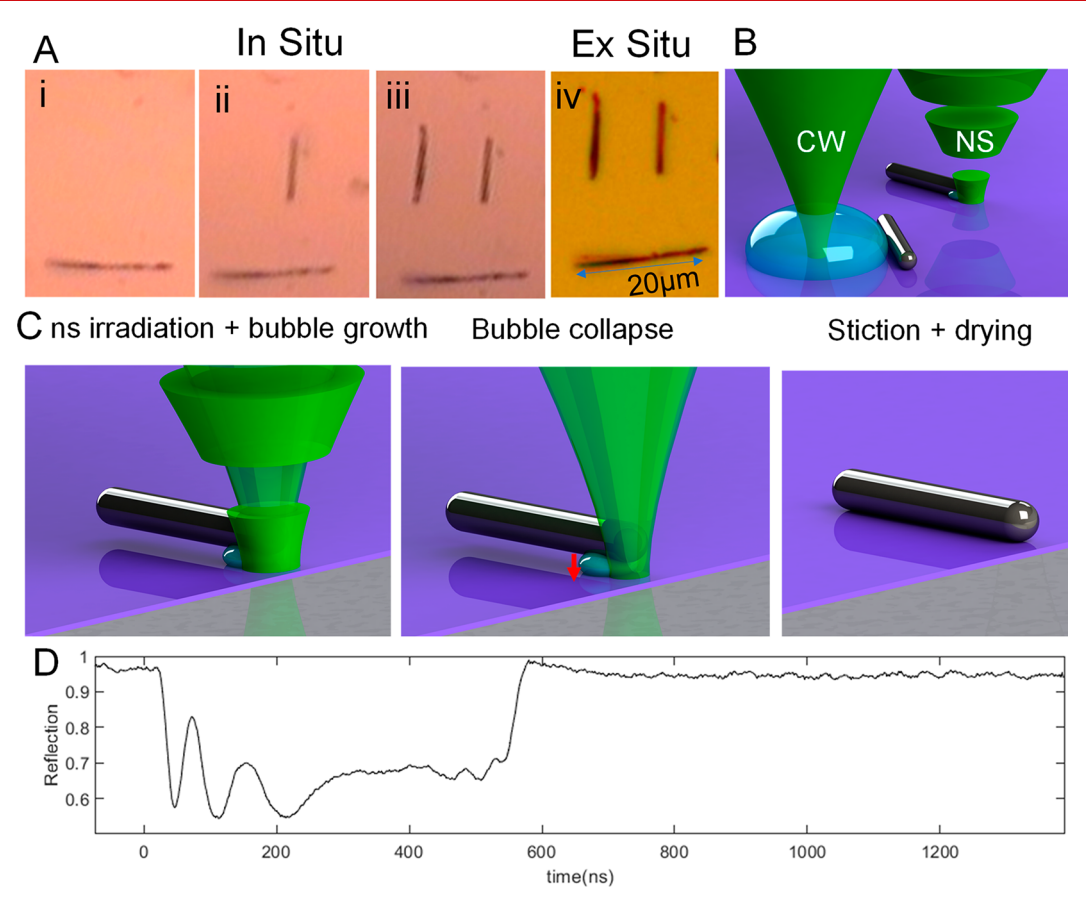


Figure 4. Positioning and stiction of silicon nanowires. (A) Sequential imaging of the assembly and drying of three SiNW's into a simple face shape showing deterministic positioning and stiction, using the nanosecond laser to stick SiNWs to the substrate in i–iii; iv shows the shape after drying. (B) Illustration of difficulty in CW laser stiction vs nanosecond laser stiction, with the larger CW vapor region moving the SiNW from its desired position. (C) Illustration of proposed mechanism for nanosecond laser adhesion using nanoscale phase change to limit SiNW motion. (D) Reflected signal from SiNW during nanosecond laser stiction showing vapor phase growth and collapse, after which SiNW remains stuck to the surface.

substrate was then evaporatively dried, which did not further move the SiNW. Because the laser heating is well below the fluence levels required to melt the nanowire, the stiction cannot be caused by welding. Therefore, it was deduced that a gaseous layer was generated over the irradiated wire surface and between the wire and the substrate surface, bringing the two very close, where the van der Waals forces dominate. After the vapor phase collapses, the wire adheres to the surface throughout the later drying step via the van der Waals force.¹² The accurate stiction could not be performed with the tweezing CW laser because the surface tension and vapor momentum transfer forces from the large CW laser-induced bubble dominate the optical forces, moving the nanowire from its intended alignment. This is diagrammed in Figure 4b. We could not reduce the size of this bubble below 10 μ m by modulating the CW beam power. The reason for this is believed to be closely tied to the kinetics of bubble nucleation and growth in superheated liquids; ¹⁷ however, a comprehensive analysis of these phenomena was beyond the scope of this work. Because of the energy limit on the nanosecond laser pulse, the vapor phase forms and collapses on nanosecond time scales and is therefore of a much smaller extent and does not interfere with the positioning of the wire. This small extent of the vapor phase region is consistent with previous investigation. 18 Additionally, we know from the FDTD simulation that a large portion of the 532 nm light irradiated to the top of

the wire will be confined under the wire, so we have good reason to presume we can induce evaporation and bring the wire into contact with the substrate as diagrammed in Figure 4c.

We tuned the nanosecond laser fluence below the damage threshold of the silicon film to a fluence of 0.04 j/cm². To verify the rapid vapor phase formation, we performed a CW laser probing experiment with a 633 nm CW laser targeting the wire while it was being attached to the surface of the thin film, and the results are shown in Figure 4d. The setup for this experiment was described previously. 11 Once the nanosecond beam irradiates the SiNW, there is a sharp drop in reflectance due to the disturbance of the probe laser coupling by the small layer of vapor surrounding the wire. There are some fluctuations in the reflectance, which is expected for a rapidly expanding and contracting vapor phase; then the signal completely recovers to its initial value, indicating the full collapse of the vapor. The entire process is completed in nearly 600 ns, confirming the rapidity of the transient vapor phase expansion and collapse processes. A previous study has shown nanosecond laser vapor bubble growth on the order of 1 m/ s, 18 which would put the vapor phase on the order of 300 nm in size, much smaller in extent than the CW bubble formation. To demonstrate the precision in position and angle of the trapping and stiction process, we consecutively brought SiNWs into frame to form a simple three-line face shape as imaged in

Figure 4a. The first wire in Figure 4a,i was brought into screen from left to right, then the following two from top down in Figure 4a,ii—iii. In Figure 4a,iv, the structure was dried and imaged via a microscope. We therefore confirm that we can two-dimensionally translate, orient, and deterministically adhere silicon nanowires to a surface using low trapping power and low numerical aperture optics at 532 nm.

3. CONCLUSION

The laser tweezing of one-dimensional (1D) nanostructures has previously been attempted with dedicated optical setups employing custom optics and beam shaping. Additionally, the high laser power required makes it difficult to incorporate in systems where there may be absorbers that cause laser-induced heating, boiling, or other damage to the nanowires. Here, we have described a new approach to the laser tweezing that takes advantage of the near field optical behavior to get an order of magnitude decrease in laser power required for optical trapping combined with an increase in scanning speed. We show that we can deterministically move and orient SiNWs and then use nanosecond laser irradiation to rigidly stick them to a surface such that it will withstand drying. The critical area of further work will be to investigate tweezing of other 1D nanostructures. Since we observe an order of magnitude increase in trapping force, it may be possible to trap other metallic nanowires or multiwalled carbon nanotubes more easily. Additionally, because the radiation travels primarily in the gap between the substrate/film and the solid nanostructure, the optical properties of the nanowire and film itself should play a smaller role. Therefore, we would expect to be able to trap absorptive and reflective particles with similar efficiency to that of the high refractive index SiNW and silver nanowires on films or substrates other than thin film a-Si and aluminum. Finally, the stability and relative simplicity of this work implies that the use of laser tweezing may have further device level applications providing fresh areas of application to bottom-up technologies.

ASSOCIATED CONTENT

Supporting Information

We include as Supporting Information all videos referenced in the text, including videos of the tweezing of nanowires at varied parameters and videos of the simulated electric fields. We also include additional cross-sectional images of the electric fields for reference, and further description of the simulations and how outputs were calculated. The Supporting Information is available free of charge at https://pubs.acs.org/doi/10.1021/acs.nanolett.2c00834.

Video of the laser tweezing at 5 mW power and 30 μ m/s translation rate (MP4)

Video of the laser tweezing at 5 mW power and 15 μ m/s translation rate, wires are scanned off the a-Si film to demonstrate nozzling effect (MP4)

Video of the laser tweezing at 5 mW power and 15 μ m/s translation rate, wires are scanned off the a-Si film to demonstrate nozzling effect (MP4)

Video of the laser tweezing for single SiNW at 6 mW power and 15 μ m/s translation rate (MP4)

Video of the laser tweezing for single silver nanowire at 6 mW power and 60 μ m/s translation rate (MP4)

Video of the laser tweezing for single SiNW at 6 mW power and 10 μ m/s translation rate performed on an aluminum film surface (MP4)

Video of electric field magnitude output of simulation from a plane parallel to the substrate and between the substrate and the SiNW (MP4)

Video of electric field magnitude output of simulation from a plane perpendicular to the substrate and bisecting the SiNW through its cylindrical axis (MP4)

Additional cross-sectional images of the electric fields for reference and a further description of the simulations and how outputs were calculated (PDF)

AUTHOR INFORMATION

Corresponding Author

Costas P. Grigoropoulos — University of California— Berkeley, Berkeley, California 94720-1740, United States; orcid.org/0000-0002-8505-4037; Phone: +1-510-642-2525; Email: cgrigoro@berkeley.edu

Author

Matthew Eliceiri — University of California—Berkeley, Berkeley, California 94720-1740, United States

Complete contact information is available at: https://pubs.acs.org/10.1021/acs.nanolett.2c00834

Author Contributions

M.E. designed experiments, performed and analyzed experiments, performed and analyzed simulations, and wrote and edited the manuscript. C.G. designed experiments, analyzed experiments, analyzed simulations, and wrote and edited the manuscript.

Notes

The authors declare no competing financial interest.

ACKNOWLEDGMENTS

The authors thank Dr. Penghong Ci and Professor Junqiao Wu of Materials Science and Engineering at UC Berkeley for supplying SiNWs for the laser tweezing. M.E. acknowledges support by a U.S. National Science Foundation Graduate Research Fellowship. Partial support of this work was also provided by the U.S. National Science Foundation under Grant CMMI-2024391.

ABBREVIATIONS

SiNW = silicon nanowire

CW = continuous wave

a-Si = amorphous silicon

FDTD = finite difference time domain

REFERENCES

- (1) Ashkin, A.; Dziedzic, J. M.; Bjorkholm, J. E.; Chu, S. Observation of a single-beam gradient force optical trap for dielectric particles. *Opt. Lett.* **1986**, *11*, 288–290.
- (2) Juan, M. L.; Righini, M.; Quidant, R. Plasmon nano-optical tweezers. *Nat. Photonics* **2011**, *5*, 349–356.
- (3) Kotnala, A.; Zheng, Y. Digital Assembly of Colloidal Particles for Nanoscale Manufacturing. *Part. Part. Syst. Charact.* **2019**, *36*, 1900152.
- (4) Dienerowitz, M.; Mazilu, M.; Dholakia, K. Optical manipulation of nanoparticles: a review. *J. Nanophotonics* **2008**, *2*, 021875.
- (5) Agarwal, R.; et al. Manipulation and assembly of nanowires with holographic optical traps. *Opt. Express* **2005**, *13*, 8906.

- (6) Pauzauskie, P. J.; et al. Optical trapping and integration of semiconductor nanowire assemblies in water. *Nat. Mater.* **2006**, *S*, 97–101.
- (7) Yan, Z.; et al. Three-Dimensional Optical Trapping and Manipulation of Single Silver Nanowires. *Nano Lett.* **2012**, *12*, 5155–5161.
- (8) Holsteen, A. L.; Raza, S.; Fan, P.; Kik, P. G.; Brongersma, M. L. Purcell effect for active tuning of light scattering from semiconductor optical antennas. *Science* **2017**, *358*, 1407–1410.
- (9) Purcell, E. M.; Torrey, H. C.; Pound, R. V. Resonance Absorption by Nuclear Magnetic Moments in a Solid. *Phys. Rev.* **1946**, 69, 37–38.
- (10) Hochbaum, A. I.; et al. Enhanced thermoelectric performance of rough silicon nanowires. *Nature* **2008**, *451*, 163–167.
- (11) Wang, L.; et al. Fast Reversible Phase Change Silicon for Visible Active Photonics. *Adv. Funct. Mater.* **2020**, *30*, 1910784.
- (12) Intermolecular and Surface Forces, revised third ed.; Academic Press, 2011; pp 253–289.
- (13) Rodrigues, J. R.; Gusso, A.; Rosa, F. S. S.; Almeida, V. R. Rigorous analysis of Casimir and van der Waals forces on a silicon nano-optomechanical device actuated by optical forces. *Nanoscale* **2018**, *10*, 3945–3952.
- (14) Zhuravlev, L. T. Concentration of hydroxyl groups on the surface of amorphous silicas. *Langmuir* 1987, 3, 316–318.
- (15) Hofmann, U.; Endell, K.; Wilm, D. Röntgenographische und kolloidchemische Untersuchungen über Ton. *Angew. Chem.* **1934**, *47*, 539–547.
- (16) Metin, C. O.; Lake, L. W.; Miranda, C. R.; Nguyen, Q. P. Stability of aqueous silica nanoparticle dispersions. *J. Nanoparticle Res.* **2011**, *13*, 839–850.
- (17) Carey, V. P. Liquid Vapor Phase Change Phenomena: An Introduction to the Thermophysics of Vaporization and Condensation Processes in Heat Transfer Equipment, second ed; CRC Press, 2007; pp 169–172.
- (18) Kim, D.; Park, H. K.; Grigoropoulos, C. P. Interferometric probing of rapid vaporization at a solid—liquid interface induced by pulsed-laser irradiation. *Int. J. Heat Mass Transfer* **2001**, *44*, 3843—3853.
- (19) Thutupalli, G. K. M.; Tomlin, S. G. The optical properties of amorphous and crystalline silicon. *J. Phys. C Solid State Phys.* **1977**, *10*, 467–477.